Supplemental materials - Intrinsic long range antiferromagnetic coupling in dilutely V doped $CuInTe_2$

Weiyi Gong, Ching-Him Leung, Chuen-Keung Sin, Jingzhao Zhang, Xiaodong Zhang, Bin Xi, and Junyi Zhu*
Department of Physics, The Chinese University of Hong Kong, Hong Kong SAR, China

CALCULATION SETUP AND CONVERGENCE TEST

All calculations were performed using projected augmented plane wave method[1] and density functional theory with Perdew-Burke-Ernzerhof generalized gradient approximation(GGA) [2] as implemented in VASP code[3]. The V doped $CuInTe_2$ was simulated in $2\times2\times1$ supercell and $3\times3\times1$ supercell. Atoms were relaxed with force tolerance of 0.01 eVÅ^{-1}. A plane wave energy cutoff of 300 eV was used in all calculations. The Brillouin zone integrations were performed by using Γ centered $5\times5\times5$ k-points grid. The convergence test of energy of the system using different number of k points was shown in figure 1.

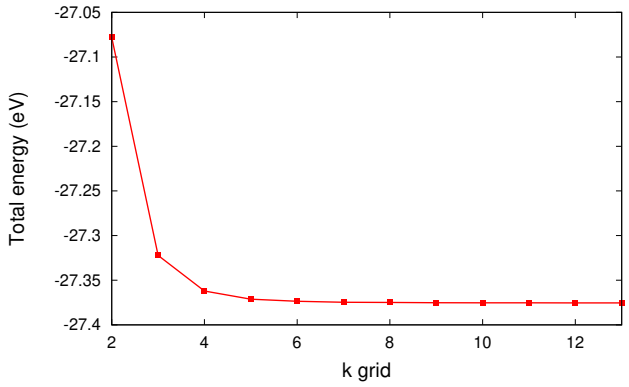

FIG. 1. The convergence test of k grid. For each i in the horizontal axis, the k grid is $i\times i\times i$.

A strong correlation effect was considered for transition metal, and DFT+U method was used[4]. We chose the onsite Coulomb interaction parameter $U = 4.70$ eV and onsite exchange interaction $J = 0.70$ eV, so that effective parameter $U_{\text{eff}} = 4.00$ eV, as suggested in Ref.[5]. In order to explore the short range and long range magnetic coupling, we substituted two In or Ga atoms with two V atoms with increasing distance.

* jyzhu@phy.cuhk.edu.hk

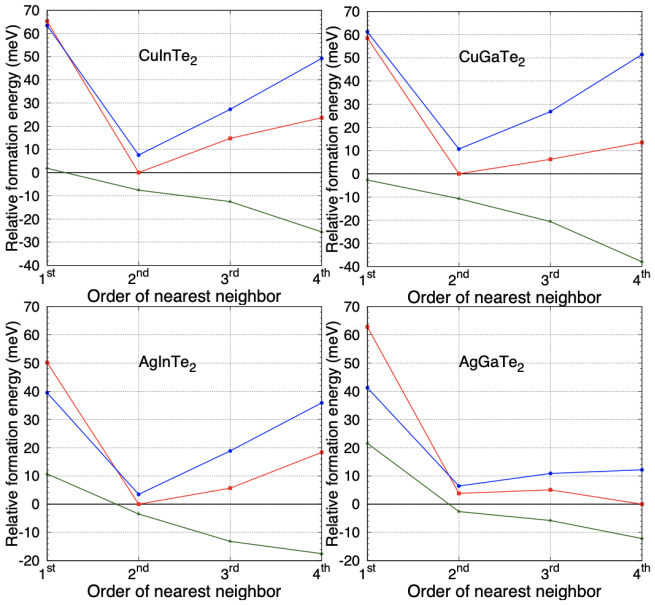

FIG. 2. The relative formation energy of the four systems with two V doped into as a function of various neighboring configurations. Red(Blue) represents the energy of AFM(FM) configurations, and green ones are their differences. Here AFM(FM) are defined as two V atoms have antiparallel(parallel) spins.

CALCULATIONS IN $CuGaTe_2$, $AgGaTe_2$ AND $AgInTe_2$

The relative formation energies of V doped $ABTe_2$ as a function of different neighboring configurations were calculated from fully relaxed $2\times2\times1$ supercell, shown in Fig.2. As shown in the Fig.2, the second NN AFM state is the global minimum in the $CuInTe_2$, $CuGaTe_2$ and $AgInTe_2$, while lowest energy configuration in $AgGaTe_2$ is the forth nearest neighbor. V doped $CuInTe_2$ has an AFM-FM energy difference 5.81 meV. The relative formation energy difference between the first NN and second NN are similar in both $2\times2\times1$ and $3\times3\times1$ supercells. Hence, subsequent calculation results of density of states and spin texture were illustrated in $2\times2\times1$ supercell in one of the systems, $CuInTe_2$.

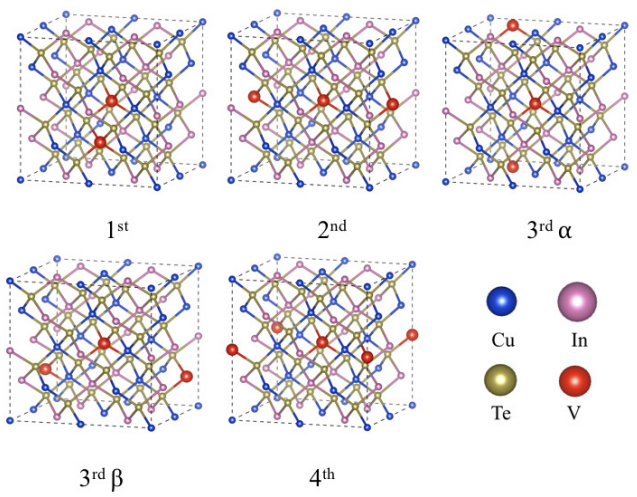

FIG. 3. The nearest neighboring configurations of two V atoms doped into the $2 \times 2 \times 1$ supercell.

CALCULATIONS IN $2 \times 2 \times 1$ SUPERCELL

The calculation setup in $2 \times 2 \times 1$ supercell was the same as stated in the main text. An In atom at body center of the supercell was substituted with a V atom. Another V atom replaces an In atom at various neighboring sites to the center V atom, from the first nearest neighbor(NN) to the forth NN, as shown in Fig.3. Cu, V and In atoms have approximately local T_d symmetry in the host cell, which is a property of chalcopyrite. The point group of this supercell is $\bar{4}2d$ (D_{2d}). Under this symmetry, the third NN has two nonequivalent configurations, while other three have only one configuration for each. Due the limitation of calculation resources, SOC calculation was only done in $2 \times 2 \times 1$ supercell. The relative formation energy without and with SOC is shown in FIG.4.

Although the effect of spin orbit coupling (SOC) is ignored in the theoretical model in the main text, SOC may induce further splitting of energy levels of heavy atoms like Te. Due to the SOC effect, the p level of Te will become lower, while this effect at Cu and In atoms is not so obvious. Hence, according to the perturbation theory, smaller energy difference will cause a larger magnetic coupling. The results of DFT calculation with SOC effect considered confirmed this point. At the second nearest neighbor, AFM has energy 7.57 meV lower than that of FM without SOC effect, while this value becomes 10.74 meV with SOC considered. Although the magnetic coupling of the first NN changes from FM to AFM once SOC is considered, the general trends of formation energy as functions of neighboring sites are similar.

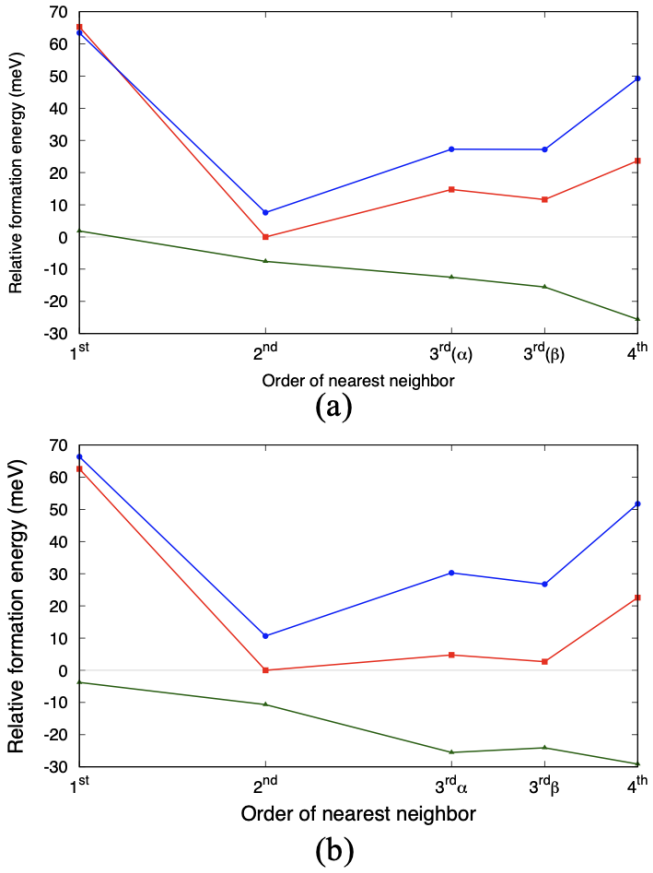

FIG. 4. The relative formation energy in $2 \times 2 \times 1$ supercell. (a) without SOC; (b) with SOC. Red(blue) line represents the formation energy of AFM(FM) configuration, green line represents their difference.

CALCULATIONS IN $3 \times 3 \times 1$ SUPERCELL

The setup is the same as above, but there are more NN configurations. In FIG.6, In atoms are labeled by (n, m), where n is the label of cell and m is the label of In atom. In the magnetic doping process, two In atoms are replaced by two V atoms. Due to the symmetry in chalcopyrite, we fix one V atom at position (1, 6). The position of the second V atom is shown in Tab.I.

TABLE I. The positions of the second V atom.

NN	1	2	3	4	5	6
position	(2, 8)	(2, 6)	(5, 1) or (5, 3)	(5, 6)	(3, 8)	(6, 1)
V-V distance(Å)	4.38	6.19	7.58	8.75	9.79	11.59

The setup of calculation in $3 \times 3 \times 1$ supercell was the same as that of $2 \times 2 \times 1$ supercell. Static calculation with SOC was performed to qualitatively check the effect of SOC. The results without and with static SOC

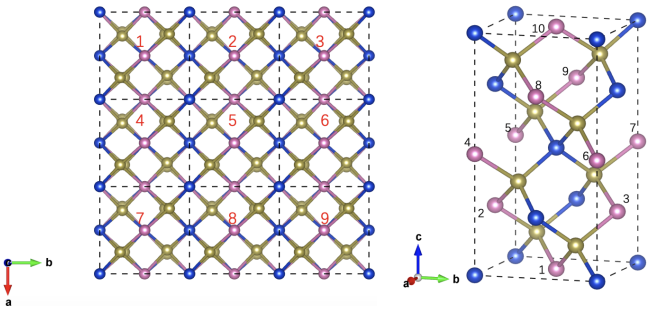

FIG. 5. The nearest neighboring configurations of two V atoms doped into the $3 \times 3 \times 1$ supercell.

calculation were shown in FIG.6. The general trends of the formation energy and energy difference between FM and AFM are similar. We see that the second NN is still the most stable configuration in larger supercell without SOC, while the stability of the sixth NN is comparable with that of the second NN. The formation energy is determined both by magnetic coupling strength and the local stress that may slightly vary with or without SOC. Nevertheless, the stabilization of long range configurations versus the first nearest neighboring configuration is valid for both setup.

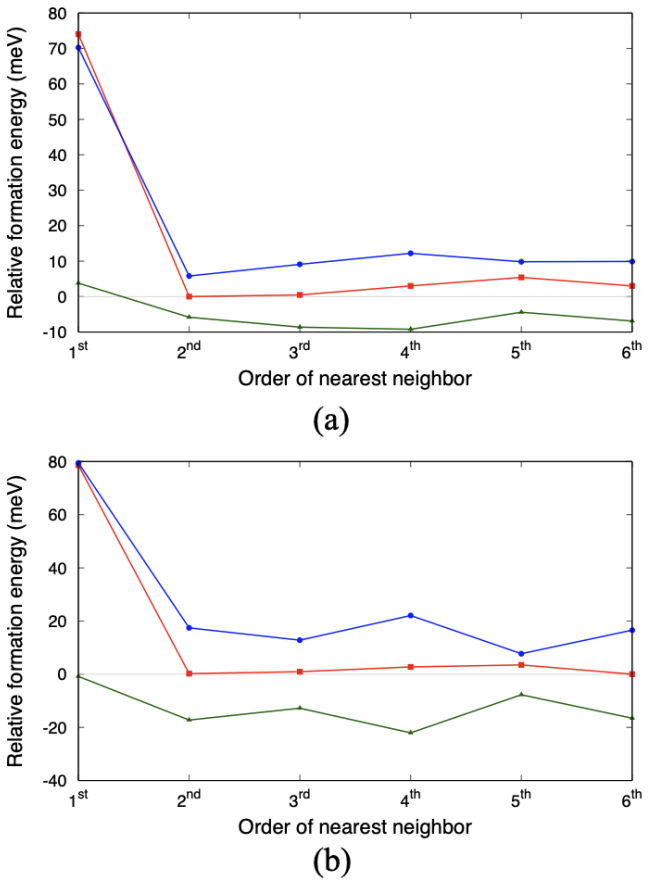

FIG. 6. The relative formation energy in $3 \times 3 \times 1$ supercell. (a) without SOC; (b) with SOC. Red(blue) line represents the formation energy of AFM(FM) configuration, green line represents their difference.

NORMAL ORDERING OF LOCAL OPERATORS

The electron number operator, onsite hopping and local magnetic moment operator at each site are defined as:

$$\begin{aligned} \hat{n} &= \sum_{\alpha\sigma} \hat{c}^{\dagger}_{\alpha\sigma}\hat{c}_{\alpha\sigma} = \sum_{\sigma} \hat{n}_{\alpha\sigma}, \\ \hat{n}_{\alpha\beta} &= \sum_{\sigma} \hat{c}^{\dagger}_{\alpha\sigma}\hat{c}_{\beta\sigma}, \\ \hat{\boldsymbol{m}} &= \sum_{\alpha\sigma\sigma'} \hat{c}^{\dagger}_{\alpha\sigma}\boldsymbol{\tau}_{\sigma\sigma'}\hat{c}_{\alpha\sigma'}, \\ \boldsymbol{\tau}_{\sigma\sigma'} &= (\tau^{x}_{\sigma\sigma'}, \tau^{y}_{\sigma\sigma'}, \tau^{z}_{\sigma\sigma'}), \end{aligned} \tag{1}$$

where α, β are indices of local orbitals, σ, σ' are indices for spins and τ^x, τ^y, τ^z are three Pauli matrices. The normal ordering of $\hat{n}^2$ and $\hat{n}^2_{\alpha\beta}$ are defined as:

$$\begin{aligned} :\hat{n}^2: &= \sum_{\alpha\beta\sigma\sigma'} \hat{c}^{\dagger}_{\alpha\sigma}\hat{c}^{\dagger}_{\beta\sigma'}\hat{c}_{\beta\sigma'}\hat{c}_{\alpha\sigma} \\ &= -\sum_{\alpha\beta\sigma\sigma'} \hat{c}^{\dagger}_{\alpha\sigma}(\delta_{\alpha\beta}\delta_{\sigma\sigma'} - \hat{c}_{\alpha\sigma}\hat{c}^{\dagger}_{\beta\sigma'})\hat{c}_{\beta\sigma'} \\ &= -\hat{n} + \hat{n}^2, \end{aligned} \tag{2}$$

and

$$\begin{aligned} :\hat{n}^2_{\alpha\beta}: &= \sum_{\sigma\sigma'} \hat{c}^{\dagger}_{\alpha\sigma}\hat{c}^{\dagger}_{\alpha\sigma'}\hat{c}_{\beta\sigma'}\hat{c}_{\beta\sigma} \\ &= -\sum_{\sigma\sigma'} \hat{c}^{\dagger}_{\alpha\sigma}(\delta_{\alpha\beta}\delta_{\sigma\sigma'} - \hat{c}_{\beta\sigma}\hat{c}^{\dagger}_{\alpha\sigma'})\hat{c}_{\beta\sigma'} \\ &= -\hat{n}_{\alpha\beta}\delta_{\alpha\beta} + \hat{n}^2_{\alpha\beta}. \end{aligned} \tag{3}$$

Note that $[\hat{n}_{\alpha\sigma}, \hat{n}_{\alpha\sigma'}] = 0$ and $\hat{n}^2_{\alpha\sigma} = \hat{n}_{\alpha\sigma}$, so we have:

$$\begin{aligned} \hat{n}^2_{\alpha} &= (\hat{n}_{\alpha\uparrow} + \hat{n}_{\alpha\downarrow})^2 \\ &= \hat{n}^2_{\alpha\uparrow} + \hat{n}^2_{\alpha\downarrow} + \hat{n}_{\alpha\uparrow}\hat{n}_{\alpha\downarrow} + \hat{n}_{\alpha\downarrow}\hat{n}_{\alpha\uparrow} \\ &= \hat{n}_{\alpha\uparrow} + \hat{n}_{\alpha\downarrow} + 2\hat{n}_{\alpha\uparrow}\hat{n}_{\alpha\downarrow}. \end{aligned} \tag{4}$$

Combining (3) and (4) gives us:

$$\begin{aligned} \sum_{\alpha\beta} :\hat{n}^2_{\alpha\beta}: &= -\sum_{\alpha} \hat{n}_{\alpha} + \sum_{\alpha\beta} \hat{n}^2_{\alpha\beta} \\ &= -\hat{n} + \sum_{\alpha} \hat{n}^2_{\alpha} + \sum_{\alpha\neq\beta} \hat{n}^2_{\alpha\beta} \\ &= 2\sum_{\alpha} \hat{n}_{\alpha\uparrow}\hat{n}_{\alpha\downarrow} + \sum_{\alpha\neq\beta} \hat{n}^2_{\alpha\beta}. \end{aligned} \tag{5}$$

Using the relation $\boldsymbol{\tau}_{\sigma\sigma'} \cdot \boldsymbol{\tau}_{\zeta\zeta'} = 2\delta_{\sigma\zeta'}\delta_{\sigma'\zeta} - \delta_{\sigma\sigma'}\delta_{\zeta\zeta'}$, we have:

$$\begin{aligned}\hat{\boldsymbol{m}}^2 &= \sum_{\alpha\sigma\sigma'}\sum_{\beta\zeta\zeta'} \boldsymbol{\tau}_{\sigma\sigma'} \cdot \boldsymbol{\tau}_{\zeta\zeta'} \hat{c}^\dagger_{\alpha\sigma}\hat{c}_{\alpha\sigma'}\hat{c}^\dagger_{\beta\zeta}\hat{c}_{\beta\zeta'} \\ &= 2\sum_{\alpha\beta\sigma'\sigma} \hat{c}^\dagger_{\alpha\sigma}\hat{c}_{\alpha\sigma'}\hat{c}^\dagger_{\beta\sigma}\hat{c}_{\beta\sigma'} - \hat{n}^2.\end{aligned} \tag{6}$$

Note that the z component of magnetic moment operator satisfies:

$$\begin{aligned}\hat{m}_z &= \sum_\alpha (\hat{n}_{\alpha\uparrow} - \hat{n}_{\alpha\downarrow}), \\ \hat{n}^2 + \hat{m}_z^2 &= 2\sum_{\alpha\beta}(\hat{n}_{\alpha\uparrow}\hat{n}_{\beta\uparrow} + \hat{n}_{\alpha\downarrow}\hat{n}_{\beta\downarrow}).\end{aligned} \tag{7}$$

Combining (6) and (7) gives us:

$$\hat{m}^2 = \hat{m}_z^2 + 2\sum_{\alpha\beta\sigma} \hat{c}^\dagger_{\alpha\sigma}\hat{c}_{\alpha,-\sigma}\hat{c}^\dagger_{\beta,-\sigma}\hat{c}_{\beta\sigma}. \tag{8}$$

The $\alpha = \beta$ terms in the above sum is :

$$\begin{aligned}&2\sum_\alpha (\hat{c}^\dagger_{\alpha\uparrow}\hat{c}_{\alpha\downarrow}\hat{c}^\dagger_{\alpha\downarrow}\hat{c}_{\alpha\uparrow} + \hat{c}^\dagger_{\alpha\downarrow}\hat{c}_{\alpha\uparrow}\hat{c}^\dagger_{\alpha\uparrow}\hat{c}_{\alpha\downarrow}) \\ &= 2\sum_\alpha [\hat{n}_{\alpha\uparrow}(1-\hat{n}_{\alpha\downarrow}) + \hat{n}_{\alpha\downarrow}(1-\hat{n}_{\alpha\uparrow})] \\ &= 2\hat{n} - 4\sum_\alpha \hat{n}_{\alpha\uparrow}\hat{n}_{\alpha\downarrow},\end{aligned} \tag{9}$$

so

$$\hat{\boldsymbol{m}}^2 = \hat{m}_z^2 + 2\sum_{\alpha\neq\beta,\sigma} \hat{c}^\dagger_{\alpha\sigma}\hat{c}_{\alpha,-\sigma}\hat{c}^\dagger_{\beta,-\sigma}\hat{c}_{\beta\sigma} + 2\hat{n} - \sum_\alpha \hat{n}_{\alpha\uparrow}\hat{n}_{\alpha\downarrow}. \tag{10}$$

And the normal ordering of $\hat{\boldsymbol{m}}^2$ is:

$$\begin{aligned}:\hat{\boldsymbol{m}}^2: &= 2\sum_{\alpha\beta\sigma\sigma'} \hat{c}^\dagger_{\alpha\sigma}\hat{c}^\dagger_{\beta\sigma'}\hat{c}_{\beta\sigma}\hat{c}_{\alpha\sigma'} - :\hat{n}^2: \\ &= -2\sum_{\alpha\beta\sigma\sigma'} \hat{c}_{\alpha\sigma}(\delta_{\alpha\beta} - \hat{c}_{\alpha\sigma'}\hat{c}^\dagger_{\beta\sigma'})\hat{c}_{\beta\sigma} - \hat{n}^2 + \hat{n} \\ &= -2\sum_{\alpha\sigma\sigma'} \hat{c}^\dagger_{\alpha\sigma}\hat{c}_{\alpha\sigma} + \hat{\boldsymbol{m}}^2 + \hat{n} \\ &= -3\hat{n} + \hat{\boldsymbol{m}}^2.\end{aligned} \tag{11}$$

Finally, all the normal ordering of local operators have been expressed using local operators in equation (2), (5), (10) and (11).

INTERACTING HAMILTONIAN FOR P AND D ORBITALS

The electron-electron interaction for d orbitals can be expressed as[6]:

$$\begin{aligned}\hat{V} = \frac{1}{2}[&(U - \frac{1}{2}J + 5\Delta J) :\hat{n}^2: - \frac{1}{2}(J - 6\Delta J) :\hat{\mathbf{m}}^2: \\ &+ (J - 6\Delta J)\sum_{\alpha\beta} :(\hat{n}_{\alpha\beta})^2:],\end{aligned} \tag{12}$$

where the quadrupole moment operator has been ignored since ΔJ is approximately of magnitude one order lower than that of J[7]. The interaction for p orbitals can be obtained be setting $\Delta J = 0$.

U is the Coulomb interaction between t_{2g} orbitals, J is the average exchange splitting of e_g and t_{2g} orbitals and ΔJ is the difference of exchange splitting between e_g and t_{2g} orbitals. Using the conventional indices (1,2,3,4,5) to represent d orbitals $(3z^2 - r^2, zx, yz, xy, x^2 - y^2)$, respectively, the parameters can be written as:

$$\begin{aligned}U &= V_{23,23}, \\ J &= \frac{1}{2}(V_{15,51} + V_{23,32}), \\ \Delta J &= V_{15,51} - V_{23,32}.\end{aligned} \tag{13}$$

Plug equations (2), (11) and (5) into (12), we have:

$$\hat{V} = \hat{V}_0 + \hat{V}_{sf} + \hat{V}_{ph}, \tag{14}$$

where $\hat{V}_0$, spin flipping terms $\hat{V}_{sf}$ and pair hopping terms $\hat{V}_{ph}$ are given by:

$$\begin{aligned}\hat{V}_0 &= u\hat{n}^2 - v\hat{m}_z^2 - (u-v)\hat{n} + 8v\sum_\alpha \hat{n}_{\alpha\uparrow}\hat{n}_{\alpha\downarrow}, \\ \hat{V}_{sf} &= -2v\sum_{\alpha\neq\beta,\sigma} \hat{c}^\dagger_{\alpha\sigma}\hat{c}_{\alpha,-\sigma}\hat{c}^\dagger_{\beta,-\sigma}\hat{c}_{\beta\sigma}, \\ \hat{V}_{ph} &= 2v\sum_{\alpha\neq\beta}(\hat{n}_{\alpha\beta})^2 \\ &= -2v\sum_{\alpha\neq\beta,\sigma} \hat{c}^\dagger_{\alpha\sigma}\hat{c}^\dagger_{\alpha,-\sigma}\hat{c}_{\beta\sigma}\hat{c}_{\beta,-\sigma},\end{aligned} \tag{15}$$

where site label is omitted for simplicity. The parameters u, v in equation (15) are defined as:

$$\begin{aligned}u &= \frac{1}{2}U - \frac{1}{4}J + \frac{5}{2}\Delta J, \\ v &= \frac{1}{4}J - \frac{3}{2}\Delta J.\end{aligned} \tag{16}$$

Now the Hamiltonian of multi-orbital Hubbard model under tight binding approximation is:

$$\begin{aligned}\hat{H} &= \hat{H}_t + \hat{H}_e + \hat{H}_{int}, \\ &= \sum_{\langle i,j\rangle}\sum_{\alpha\beta\sigma} t^{ij}_{\alpha\beta}\hat{c}^\dagger_{i\alpha\sigma}\hat{c}_{j\beta\sigma} + h.c. \\ &+ \sum_{i\alpha\sigma} \epsilon_{i\alpha}\hat{c}^\dagger_{i\alpha\sigma}\hat{c}_{i\alpha\sigma} + \sum_i \hat{V}^i,\end{aligned} \tag{17}$$

where the hopping integrals are only nonzero between nearest neighbor atomic levels and their magnitudes and signs are discussed in the next section. $\hat{V}^i$ is the interacting Hamiltonian of each site according to equation (14).

THE HOPPING INTEGRALS

The p and d orbitals are irreducible representation of spherical symmetry with angular momentum $l = 1$ and $l = 2$. However, in a local environment with T_d symmetry, which is the local symmetry of V atoms and Cu atoms in our case, some of atomic orbitals become reducible, and will split according to the group theory. As shown in table II, there are 5 irreducible representations of T_d group, and $p(l = 1)$ and $d(l = 2)$ become reducible and split into linear combination of the irreducible representations.

TABLE II. The character table of T_d group.

T_d	E	$8C_3$	$3C_2$	$6\sigma_d$	$6S_4$
A_1	1	1	1	1	1
A_2	1	1	1	-1	-1
E	2	-1	2	0	0
T_1	3	0	-1	-1	1
T_2	3	0	-1	1	-1
Γ_p	3	0	-1	1	-1
Γ_d	5	-1	1	1	-1

From the character table we get the splitting relations:

$$\Gamma_p = T_2 \tag{18}$$
$$\Gamma_d = E + T_2 \tag{19}$$

So the p orbitals in T_d symmetry only interact with t_{2g} states of d orbitals, and interact only weakly with e_g states [8]. The magnitude and signs of hopping matrix elements for each pair of p orbitals and t_{2g} orbitals can be determined by the Slater Koster matrix [9]. The magnitude is $t = V_{pd\sigma}/\sqrt{3}$, while the signs are shown in Fig. 7.

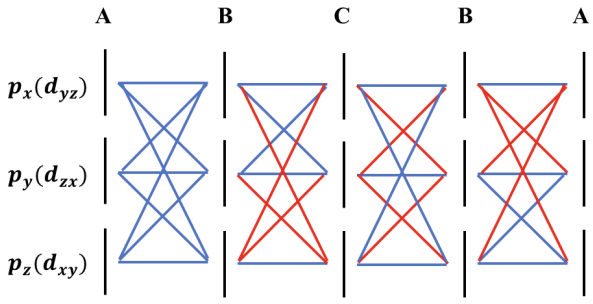

FIG. 7. The sign of hopping integrals. Black intervals represent $p_x(d_{yx}), p_y(d_{zx}), p_z(d_{xy})$ orbitals of B(A,C) atoms. Red(Blue) lines represent that the hopping integral is positive(negative) t. The chain that we chose was along the direction: A-B: (1,1,1), B-C:(1,1,-1), C-B:(-1,1,-1), B-A:(-1,1,1).

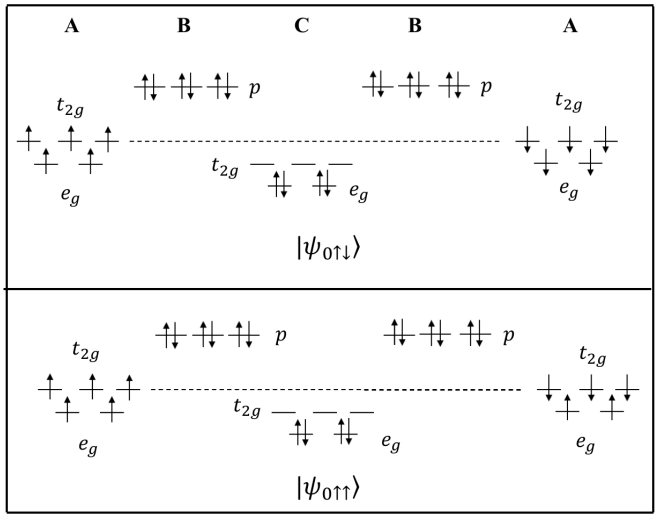

FIG. 8. The lowest energy configurations with parallel and anti-parallel spins on e_g states of site A(V).

LOW ENERGY CONFIGURATIONS

The lowest energy states with parallel($\psi_{0\uparrow\uparrow}$) and anti-parallel($\psi_{0\uparrow\downarrow}$) e_g spins at site A are shown in Fig.8.

For anti-parallel case, the lowest energy configuration has energy:

$$E_{0\uparrow\downarrow} = 4\epsilon_{A1} + 6\epsilon_{A2} + 12\epsilon_B + 4\epsilon_{C1} + 40u_A - 40v_A + 60u_B + 60v_B + 12u_C + 20v_C, \tag{20}$$

where $A1$, $C1$ and $A2$, $C2$ are corresponding e_g and t_{2g} states. In this configuration, two V(A) atoms have half-filled $3d$ orbitals, two Te(B) atoms have fully filled $5p$ orbitals and Cu(C) atom has empty t_{2g} orbitals and fully filled e_g orbitals. The spin configuration of two A atoms in this state is $3d^5_\uparrow$, $3d^5_\downarrow$ obeying the Hund's rule. Electrons on t_{2g} orbitals of A can effectively hop to t_{2g} orbitals of C mediated by p electrons on B. In this process, one B electron hop to C first, and one A electron hop to B next. The energy of intermediate states and the states after one effective hopping are:

$$E_{1\uparrow\downarrow} = E_{0\uparrow\downarrow} + 8u_C - 10u_B - 10v_B - \Delta_{BC} + \delta_C,$$
$$E_{2\uparrow\downarrow} = E_{0\uparrow\downarrow} + 8u_C - 8u_A + 8v_A - \Delta_{AC} + \delta_C - \delta_A, \tag{21}$$

where $\Delta_{AC} = \epsilon_{A1} - \epsilon_{C1}$ and $\Delta_{BC} = \epsilon_B - \epsilon_{C1}$ are energy difference between A, C and B p, C e_g states. And δ_A and δ_C are the crystal field splitting of A and C atoms. Applying the fourth order perturbation theory gives us:

$$E_{\uparrow\downarrow} = E_{0\uparrow\downarrow} - \frac{18t^2}{E_{1\uparrow\downarrow} - E_{0\uparrow\downarrow}} - \frac{18t^4}{(E_{1\uparrow\downarrow} - E_{0\uparrow\downarrow})^2(E_{2\uparrow\downarrow} - E_{0\uparrow\downarrow})}, \tag{22}$$

where the coefficients in front of each terms come from the degeneracy of p and d orbitals.

Similar procedure can be applied to parallel initial spins of V atoms. The lowest energy is:

$$E_{0\uparrow\uparrow} = 4\epsilon_{A1} + 6\epsilon_{A2} + 12\epsilon_B + 4\epsilon_{C1} + 40u_A - 16v_A + 60u_B + 60v_B + 12u_C + 20v_C. \tag{23}$$

We find that it is $24v_A$ lower than $E_{\uparrow\downarrow}$. This is because $\psi_{0\uparrow\downarrow}$ state has larger local magnetic moment and results in a smaller energy. Electrons at sites A can hop to site C via a similar effective hopping process. In the parallel case, two A atoms are asymmetric, so we denote the state after one effective hopping of an up(down) spin from t_{2g} orbitals at site A as $\psi_{2\uparrow\uparrow}(\psi'_{2\uparrow\uparrow})$. Starting from the lowest energy configuration, we listed the energies of the states with the second and forth order corrections:

$$\begin{aligned} E_{1\uparrow\uparrow} &= E'_{1\uparrow\uparrow} = E_{0\uparrow\uparrow} + 8u_C - 10u_B - 10v_B - \Delta_{BC} + \delta_C, \\ E_{2\uparrow\uparrow} &= E_{0\uparrow\uparrow} + 8u_C - 8u_A + 8v_A - \Delta_{AC} + \delta_C - \delta_A, \\ E'_{2\uparrow\uparrow} &= E_{2\uparrow\uparrow} - 8v_A. \end{aligned} \tag{24}$$

Applying the forth order perturbation theory gives us:

$$E_{\uparrow\uparrow} = E_{0\uparrow\uparrow} - \frac{18t^2}{E_{1\uparrow\uparrow} - E_{0\uparrow\uparrow}} - \frac{9t^4}{(E_{1\uparrow\uparrow} - E_{0\uparrow\uparrow})^2}\left(\frac{1}{E_{2\uparrow\uparrow} - E_{0\uparrow\uparrow}} + \frac{1}{E'_{2\uparrow\uparrow} - E_{0\uparrow\uparrow}}\right). \tag{25}$$

So the energy difference between parallel and anti-parallel e_g spins of V atoms is:

$$\begin{aligned} E_{\uparrow\uparrow} - E_{\uparrow\downarrow} &= 24v_A + \frac{9t^4}{(\Delta E_{10})^2}\left(\frac{1}{\Delta E_{20}} - \frac{1}{\Delta E_{20} - 8v_A}\right) \\ &\approx 24v_A - \frac{72t^4 v_A}{(\Delta E_{10})^2(\Delta E_{20})^2}, \end{aligned} \tag{26}$$

where $\Delta E_{10} = E_{1\uparrow\downarrow} - E_{0\uparrow\downarrow} = E_{1\uparrow\uparrow} - E_{0\uparrow\uparrow}$, $\Delta E_{20} = E_{2\uparrow\downarrow} - E_{0\uparrow\downarrow} = E_{2\uparrow\uparrow} - E_{0\uparrow\uparrow}$.

COULOMB INTERACTION ENERGY

The stability of long range AFM coupling instead of the short range superexchange may get some explanation from the simple Coulomb interaction picture. The electrostatic Coulomb potential energy between two V atoms is

$$k\frac{Ze^2}{r} = 14.404 \times \frac{Z^2}{\tilde{r}}\ eV, \tag{27}$$

where k is electrostatic constant, Z is the number of charges and $\tilde{r}$ is the distance in unit Å. If we assume the effect mainly comes from the interaction between two V atoms, the electrostatic energy difference between 1st NN and 2nd NN is

$$14.404\ eV \times \left(\sum_i Z_i^2 \frac{n_i}{\tilde{r}_i} - \sum_j Z_j^2 \frac{n_j}{\tilde{r'}_i}\right), \tag{28}$$

where the summation is taken over for all possible bonds linking to V atoms, and n is effective number of bonds. Taking the summation of bond length up to 16 Å, we get the Coulomb repulsion energy is 104 meV, which is of the same order with the calculated energy difference in Fig.2 and **??**.

ENERGY MAPPING ANALYSIS

The energy mapping analysis is a DFT computational method to extract coefficients in Heisenberg Hamiltonian with anisotropy terms by calculating the total energy of fixed spin configurations [10]. By fitting the model

$$\hat{H} = J\boldsymbol{S}_1 \cdot \boldsymbol{S}_2 + A\sum_{i=1,2}(S_i^z)^2 \tag{29}$$

we get $J \approx 3.5$ meV, $A \approx 0.5$ meV.

[1] P. E. Blöchl, Phys. Rev. B **50**, 17953 (1994).
[2] J. P. Perdew, A. Ruzsinszky, G. I. Csonka, O. A. Vydrov, G. E. Scuseria, L. A. Constantin, X. Zhou, and K. Burke, Phys. Rev. Lett. **100**, 136406 (2008).
[3] G. Kresse and J. Furthmüller, Phys. Rev. B **54**, 11169 (1996).
[4] S. L. Dudarev, G. A. Botton, S. Y. Savrasov, C. J. Humphreys, and A. P. Sutton, Phys. Rev. B **57**, 1505 (1998).
[5] Y. Zhang, J. Zhang, W. Gao, T. A. Abtew, Y. Wang, P. Zhang, and W. Zhang, J. Chem. Phys. **139**, 184706 (2013).
[6] M. E. A. Coury, S. L. Dudarev, W. M. C. Foulkes, A. P. Horsfield, P.-W. Ma, and J. S. Spencer, Phys. Rev. B **93**, 075101 (2016).
[7] A. M. Oles and G. Stollhoff, Phys. Rev. B **29**, 314 (1984).
[8] J. E. Jaffe and A. Zunger, Phys. Rev. B **29**, 1882 (1984).
[9] J. C. Slater and G. F. Koster, Phys. Rev. **94**, 1498 (1954).
[10] H. Xiang, C. Lee, H.-J. Koo, X. Gong, and M.-H. Whangbo, Dalton Trans. **42**, 823 (2013).